Available online at www.sciencedirect.com
ScienceDirect
Trans. Nonferrous Met. Soc. China 19(2009) 1464−1469
Transactions of Nonferrous Metals Society of China
www.tnmsc.cn

Martensitic transformation and mechanical properties of Ti-rich Ti-Ni-Cu melt-spun ribbon

HE Wen-jun(何文军)[1], MIN Guang-hui(闵光辉)[2], YIN Yan-sheng(尹衍升)[1], O. TOLOCHKO[3]

1. Institute of Materials Science and Engineering, Ocean University of China, Qingdao 266100, China;
2. School of Materials Science and Engineering, Shandong University, Ji'nan 250061, China;
3. Department of Material Science, Saint-Petersburg State Polytechnic University, Polytechnicheskaya Str., 29, St. Petersburg, 195251, Russia

Received 10 August 2009; accepted 15 September 2009

Abstract: Martensitic transformation, mechanical and thermomechanical properties of a Ti-rich $Ti_{52}Ni_{23}Cu_{25}$ melt spun ribbon annealed at a temperature below the crystallization temperature were studied by XRD, DSC and DMA. After annealing the initially amorphous ribbon at 400 ℃ for 10 h, the ribbon is fully crystallized and exhibits one-stage $B2 \leftrightarrow B19$ phase transformation with the temperature hysteresis of 14 ℃. The annealed ribbon is composed of $B2$, $B19$ and $B11$-TiCu phase with (001) preferential orientation. On the stress—strain curves, the rearrangement of the martensite variants and stress-induced martensitic transformation are observed below the M_f temperature and above the A_f temperature, respectively. The annealed ribbon exhibits up to 1.6% superelastic shape recovery with small stress hysteresis of 25 MPa. No flat stress-plateau is associated with the superelasticity. The annealed ribbon shows a well-defined shape memory effect during thermal cycling from −60 to 100 ℃. The transformation strain and recovery strain increase with increasing the applied external stress. Under the external stress above 150 MPa, the shape recovery strain is not sensitive to it and keeps stable at about 1.74%.

Key words: Ti-Ni-Cu alloy; melt spinning; shape memory properties; superelasticity; dynamic mechanical analysis

1 Introduction

Ti-Ni-Cu ternary shape memory alloys (SMAs) are known to exhibit unique phase transformation characteristics and shape memory properties compared with Ti-Ni binary alloys[1]. The composition sensitivity of the martensitic transformation (MT) temperature, the transformation hysteresis, the superelasticity hysteresis and the flow stress level in the martensite state can be lowered for Ti-Ni-Cu alloys via substituting Cu for Ni in Ti-Ni binary SMAs[2−4]. Unfortunately, it was found that Cu addition exceeding 10% (molar fraction) can embrittle the alloy and reduce seriously the workability as well as shape recovery strain[5−6]. This restrains the application of high Cu content Ti-Ni-Cu SMAs. In recent years, melt spinning technique has been utilized to fabricate high Cu-content Ti-Ni-Cu alloys in order to avoid the intrinsic restriction. Ti-Ni-Cu alloy ribbon can exhibit amorphous or crystalline structure dependent on melt-spinning parameters[7]. Nevertheless, as-spun amorphous Ti-Ni-Cu ribbon fabricated by using a high cooling rate shows no shape memory effect (SME). Thus, a proper thermal annealing is needed to crystallize it. Previous studies[8−10] on amorphous Ti-Ni-Cu ribbon containing high Cu content were mainly focused on the thermal-annealing dependence of the microstructure, transformation characteristics and mechanical properties. It is noted that the annealing temperature performed in most cases was above the crystallization temperature (T_c) of amorphous ribbon[9,11]. Ti-Ni-Cu ribbon annealed at temperature below T_c can introduce different but special microstructures and transformation characteristics [12−13]. MT and mechanical properties are affected not only by annealing condition, but also by the ribbon composition. To date, high Cu content Ti-Ni-Cu ribbon widely studied has been carried out in $Ti_{50}Ni_{25}Cu_{25}$ alloy, where it has equal molar ratio of Ti to (Ni+Cu). Little

Foundation item: Project (05-2-JC-76) supported by the Technological Generalship Program of Qingdao City, China; Project (20050360646) supported by National Foreign Expert Key Foundation of China
Corresponding author: YIN Yan-sheng; Tel: +86-532-66781795; Fax: + 86-532-66786385 E-mail: yys2006@ouc.edu.cn
DOI: 10.1016/S1003-6326(09)60052-2

research refers to Ti-rich or Ni-rich Ti-Ni-Cu ribbon with high Cu content[14]. To our best knowledge, the MT behavior and mechanical properties of Ti-rich Ti-Ni-Cu ribbon with high Cu content are not systematically investigated yet. In the present study, a Ti-rich $Ti_{52}Ni_{23}Cu_{25}$ (molar fraction) melt-spun ribbon is annealed to be crystallized at 400 ℃ for 10 h. Thereafter, MT behavior, mechanical and thermomechanical properties of the annealed ribbon are studied by differential scanning calorimeter (DSC) and dynamic mechanical analyzer (DMA).

2 Experimental

Ti-rich Ti-Ni-Cu melt-spun ribbon was prepared by the planar flow casting technique. Pre-synthesized $Ti_{52}Ni_{23}Cu_{25}$ alloys were prepared from the high purity metals by melting 6 times in argon arc furnace. The obtained ingots were re-molten in quartz crucibles under a purified helium atmosphere and ejected onto the surface of a fast rotating copper wheel. The wheel surface speed was 37 m/s. The ribbon has a width of 1.7 mm and a thickness of 35 μm. The ribbon was annealed in air furnace at 400 ℃ for 10 h, followed by water quenching. A TA instrument DSC Q100 was used to investigate the crystallization temperature and MT characteristics of the ribbon at a temperature rate of 10 ℃/min. The crystallization onset temperature of the as-spun ribbon is determined to be 440 ℃. A TA instrument DMA Q800 was used to investigate the shape memory behavior of the annealed ribbon under different constant stress during thermal cycling from 100 to −60 ℃. The heating and cooling rates were 5 ℃/min. A series of strain—temperature measurements under various constant stresses were carried out with one sample by varying the stress from 50 to 300 MPa. Tensile tests were carried out in the same DMA instrument in the static tensile mode to investigate the mechanical and superelasticity properties of the annealed ribbon. The specimens were heated to 100 ℃ to obtain the parent phase prior to each tensile test. In the mechanical tests, the upper limit of load and the loading rate were 18 N and 0.5 N/min, respectively. The gauge length of each specimen for thermal cycling tests and tensile tests was set to be 10 mm. X-ray diffraction patterns were taken with Cu K_α radiation to identify the phases formed in the melt-spun ribbon.

3 Results and discussion

3.1 Martensitic transformation behavior of Ti-Ni-Cu alloy ribbon

Fig.1 shows the DSC curves of the $Ti_{52}Ni_{23}Cu_{25}$ alloy ribbon during heating and cooling processes from

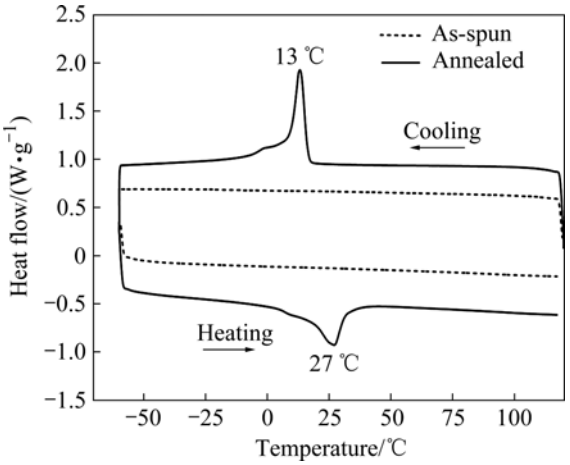

Fig.1 DSC curves of as-spun $Ti_{52}Ni_{23}Cu_{25}$ ribbon and ribbon annealed at 400 ℃ for 10 h upon cooling and heating

−60 to 120 ℃. No DSC phase transformation peaks are visible on the curve of as-spun ribbon, indicating that as-spun ribbon is fully amorphous. A amorphous material seems useless in the filed of SMAs unless it is treated with proper crystallization process. After annealing the ribbon at 400 ℃ for 10 h, there is only one-stage transformation peak during heating and cooling in the DSC curve that can be attributed to reversible MT. The corresponding transformation temperatures are as follows: M_s=17 ℃, M_f =7 ℃, A_s=14.3 ℃ and A_f=33 ℃. The transformation hysteresis between reversible MT of the annealed ribbon is defined as the difference between peak temperatures of austenite (A_p) and martensite (M_p). In Fig.1, it can be seen that the transformation hysteresis is small as 14 ℃, which is about 7 ℃ higher than that of the annealed $Ti_{50}Ni_{25}Cu_{25}$ ribbon[9].

Fig.2 shows the XRD patterns of as-spun ribbon and the annealed ribbon. Only a hump of very low intensity in the XRD spectrum of as-spun ribbon was observed, showing that an amorphous structure exists in the as-spun ribbon, as shown in Fig.2(a). As the ribbon was

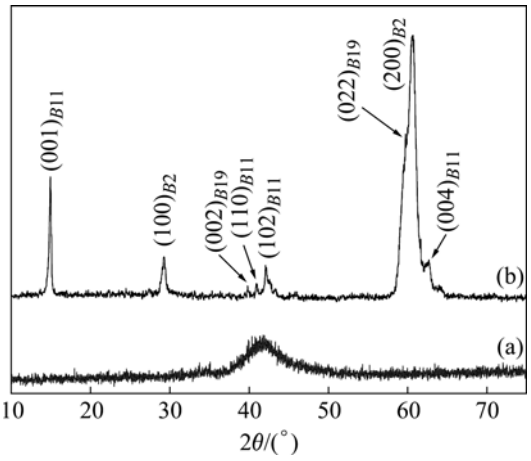

Fig.2 XRD patterns of $Ti_{52}Ni_{23}Cu_{25}$ alloy ribbon: (a) As-spun; (b) Annealed at 400 ℃ for 10 h

annealed at 400 ℃ for 10 h, it was fully crystallized although the annealing temperature is below the crystallization onset temperature. Fig.2(b) shows that *B*2 parent phase and *B*19 martensite phase exist in the annealed ribbon at room temperature. The lattice parameter of *B*2 is found to be a=0.305 nm, which is similar to that in $Ti_{50}Ni_{25}Cu_{25}$ ribbon[15]. The coexistence of *B*2 and *B*19 in the XRD pattern indicates that the annealed ribbon undergoes $B2 \leftrightarrow B19$ reversible phase transformation. Therefore, the transformation peaks during cooling and heating in Fig.2 are attributed to reversible $B2 \leftrightarrow B19$ phase transformation. Additionally, the diffraction peaks corresponding to *B*11-TiCu phase were found in the pattern. From the relative intensity of the *B*11-TiCu diffraction peaks, we can see that the preferential orientation of $(001)_{B11\text{-}TiCu}$ is developed in the annealed ribbon.

3.2 Mechanical properties of annealed ribbon

Fig.3 shows the stress—strain curves of the annealed ribbon obtained at different temperatures. In Fig.3(a), where the deformation temperatures, namely −20, −40 and −60 ℃, are below M_f temperature, several typical ferroelastic stress—strain curves are obtained. On loading, all curves can be divided into three stages. The first linear stage corresponds to the elastic deformation of the martensite phase. In the next stage, the flow stress increases slowly until the strain reaches about 1.75%. This stage corresponds to the rearrangement of the martensite variants. After the second stage finishes, the stress—strain curves become linear again. The third linear stage corresponds to the elastic deformation of the reoriented martensite. Due to the limitation of tensile force in the DMA instrument, no stage corresponds to the plastic deformation of the reoriented martensite phase.

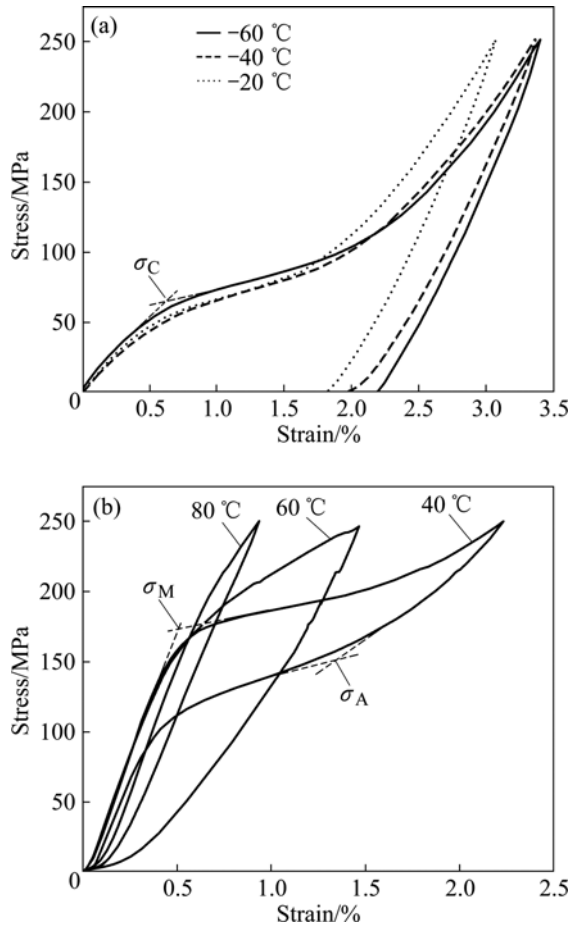

Fig.3 Stress—strain curves of $Ti_{52}Ni_{23}Cu_{25}$ ribbon annealed at 400 ℃ for 10 h at deformation temperatures measured from −60 to 80 ℃: (a) Below M_f; (b) Above A_f

Fig.3(b) shows the stress—strain curves obtained at other three temperatures, namely 40, 60 and 80 ℃, which are higher than A_f (33 ℃). On these curves, the deformation occurred on loading is recovered completely upon unloading, indicating that the annealed ribbon shows complete superelasticity. The stress—strain curve obtained at 40 ℃ is found to be divided into three stages upon loading. The first stage corresponds to the elastic deformation of the parent phase. The second stage is considered to be the stress-induced MT. In this stage, no stable flat stress plateau is associated with the stress-induced $B2 \rightarrow B19$ transformation, which is different from the superelasticity in Ti-Ni and Ti-Ni-Cu bulk materials[10]. The third stage is considered to be the elastic deformation of the stress-induced martensite. On unloading, there exists a stress region associated with reverse $B19 \rightarrow B2$ transformation. A nearly 1.6% stable shape recovery is obtained from the stress—strain loop. The stress hysteresis associated with the stress-induced $B2 \leftrightarrow B19$ transformation is defined as the difference between the stress to induce the $B2 \rightarrow B19$ transformation (σ_M) and the stress done for the $B19 \rightarrow B2$ transformation (σ_A). It is determined to be 25 MPa, as shown in Fig.3(b). The stress hysteresis associated with $B2 \leftrightarrow B19$ transformation in Ti-Ni-Cu bulk materials is 80−100 MPa[16], depending on Cu content. The stress hysteresis of the present $Ti_{52}Ni_{23}Cu_{25}$ ribbon is much smaller than that of Ti-Ni-Cu bulk materials, suggesting a highly mobile interface between martensite and austenite.

The stress—strain curve obtained at 60 or 80 ℃ is different from that at 40 ℃, although all exhibit complete superelasticity. As deformation temperature becomes higher than 60 ℃, the elastic deformation of the parent phase can be seen on the curve while the second or third stage cannot be separated clearly. This is probably because the stress-induced MT becomes difficult. The anealed ribbon shows a recoverable strain of 0.9% completely on unloading, indicating that the stress-induced MT still occurs despite the absence of a clear second stage. The curve shows a typical strain-

hardening effect by a continuous increase in stress with increasing deformation strain after the finishing of the first stage. Some factors such as grain boundaries, ordered precipitates and lattice defects originated during deformation can contribute to the strain-hardening effect [10]. As the deformation temperature increases up to 80 ℃, the critical stress to induce MT increases. The rate of strain-hardening also increases fiercely, resulting in the decrease in the maximum deformation strain from 2.23% to 0.94% compared with that at 40 or 60 ℃.

Figs.4(a) and (b) show the temperature dependence of critical stress determined by a tangential method (shown in Fig.3) and the elastic modulus of the annealed ribbon, respectively. As seen in Fig.4(a), the stress increases linearly with increasing the deformation temperature above A_f and decreases slightly with increasing the deformation temperature below M_f. The data points in Fig.4(a) can be fitted approximately by the two straight lines with the slopes of −0.16 and 0.34 MPa/℃. The difference in the temperature dependence comes from the different mechanisms. Due to the relatively low flow stress of martensite, the rearrangement of the martensite variants induced by external stress is easy. Therefore, the rearrangement of the martensite variants can be thermally activated easily. This is why the critical stress decreases slightly with increasing deformation temperature, as depicted in the first line. The second line is assumed to belong to the high-stress-induced martensitic phase. External stress can help the parent phase to transform to martensite phase in the stage corresponding to the stress-induced MT at the temperatures above the A_f temperature. As the temperature increases, the parent phase becomes stable, requiring higher critical stress to induce MT. The elastic modulii of the annealed ribbon in the martensite state and austenite state are about 12 and 37 GPa, respectively, as shown in Fig.4(b). The elastic modulus in austenite state is higher than that (about 64 GPa) of Ti-Ni wire and lower than that (about 15.4 GPa) of $Ti_{50}Ni_{25}Cu_{25}$ ribbon annealed at 500 ℃ upon loading[10]. The difference in elastic modulus between binary Ti-Ni and Ti-Ni-Cu alloy is probably due to Cu addition leading to a decrease in the atomic binding force, while the difference between the present ribbon and $Ti_{50}Ni_{25}Cu_{25}$ alloy ribbon is likely due to different texture and precipitates.

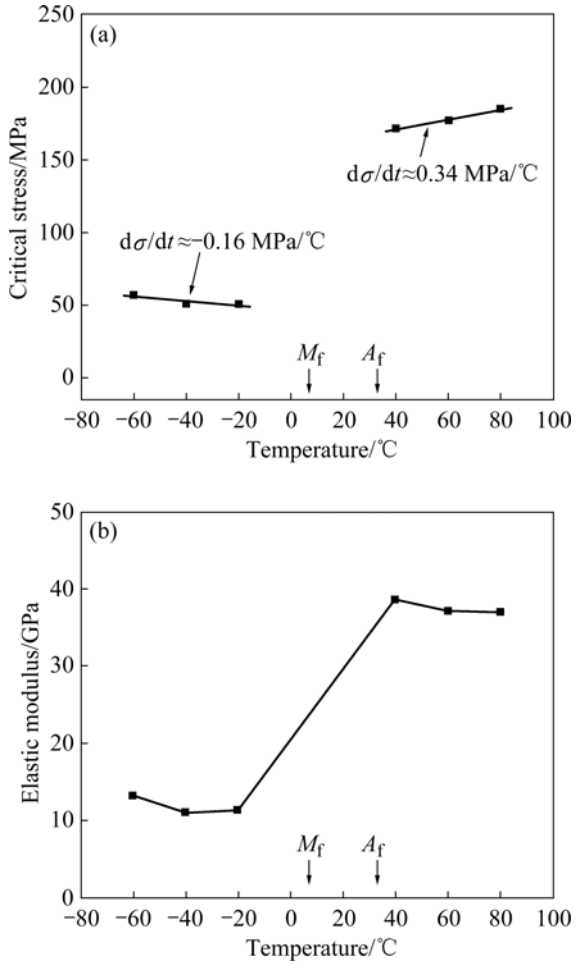

Fig.4 Critical stresses (a) and elastic modulus (b) upon loading in $Ti_{52}Ni_{23}Cu_{25}$ ribbon annealed at 400 ℃ for 10 h as function of deformation temperature

3.3 Shape memory properties of annealed ribbon

Fig.5 shows a typical example of the strain—temperature curves of $Ti_{52}Ni_{23}Cu_{25}$ alloy ribbon annealed at 400 ℃ for 10 h under various constant stresses during cooling and heating. A well-defined shape memory effect (SME) can be indicated by the elongation on cooling and shrinkage on heating during the thermal cycling. One-stage elongation and shrinkage corresponding to the reversible $B2 \leftrightarrow B19$ transformation can be found on all curves. Under a constant stress, the specimen starts to elongate due to the MT at M_s' and finishes the deformation at M_f' on cooling. While it starts to recover the deformation and shrinks due to the reverse transformation at A_s' and finishes the recovery at A_f' on

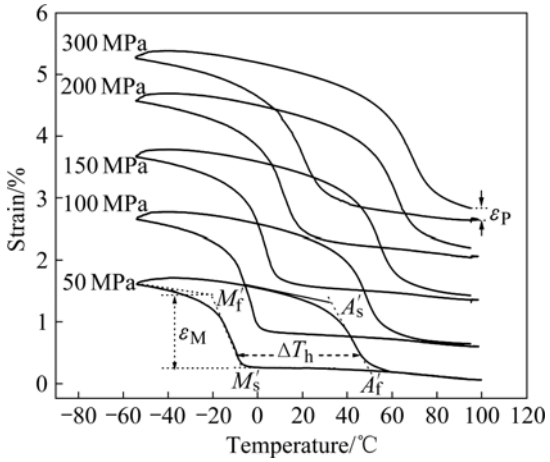

Fig.5 Strain—temperature curves under constant stress for $Ti_{52}Ni_{23}Cu_{25}$ ribbon annealed at 400 ℃ for 10 h

heating. The transformation hysteresis ΔT_h is determined by the temperature interval between the nearly parallel forward and reverse transformation curves, as shown in Fig.5.

Fig.6 shows the transformation temperatures (M_s', M_f', A_s' and A_f') and transformation hysteresis ΔT_h determined from the strain—temperature loop as a function of external constant stress in the $Ti_{52}Ni_{23}Cu_{25}$ ribbon annealed at 400 ℃ for 10 h. All transformation temperatures increase while ΔT_h decreases slowly with increasing the applied stresses. The average value of ΔT_h is about 51 ℃, which is much higher than that (14 ℃) determined by DSC under stress-free condition. The difference in the experimental instruments and the way to determine the transformation hysteresis may be partly attributed to the difference in the value of ΔT_h. Further work to analyze the difference is needed. As can be seen in Fig.6, M_s' temperature increases linearly with increasing the applied stress. The temperature dependence of the external stress to induce $B2 \longrightarrow B19$ transformation in the annealed ribbon is about 6.65 MPa/℃, which is slightly smaller than that (about 8 MPa/℃) of $Ti_{50}Ni_{25}Cu_{25}$ alloy ribbon in the previous study[17].

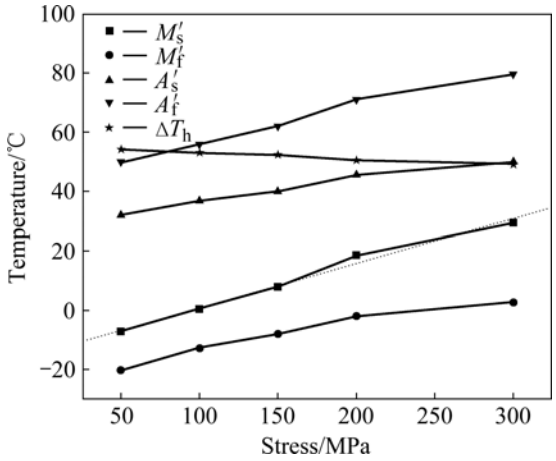

Fig.6 Transformation temperatures (M_s', M_f', A_s' and A_f') and temperature hysteresis (ΔT_h) as function of external stress for $Ti_{52}Ni_{23}Cu_{25}$ ribbon annealed at 400 ℃ for 10 h

The shape memory properties are characterized by several parameters such as the transformation strain (ε_M), the recovery strain (ε_R) and the residual strain (ε_P) determined from the strain—temperature curves. ε_M is defined as the elongation between M_s' and M_f', while ε_P originates from plastic deformation. Fig.7 shows the shape memory parameters (ε_M, ε_R and ε_P) of the annealed ribbon obtained from the strain—temperature curves (Fig.5) as a function of stress. Under a stress of 50 MPa, a shape recovery strain of about 1.13% is obtained. Its strain recovery rate equals one due to the closed strain—temperature loop as shown in Fig.5. As the stress

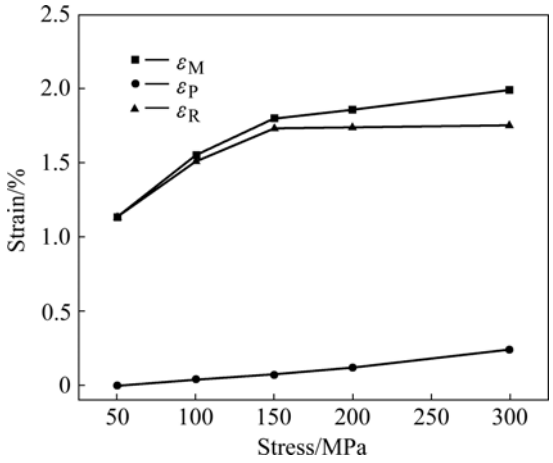

Fig.7 Transformation strain, recovery strain and plastic strain as function of external stress for $Ti_{52}Ni_{23}Cu_{25}$ ribbon annealed at 400 ℃ for 10 h

increases, the strain—temperature loop is not well closed, indicating that the plastic deformation is developed during the thermomechanical cycling. ε_M and ε_P both increase with increasing the applied stress. The maximum values of them are 1.99% and 0.24% under the maximum external stress of 300 MPa, respectively. Under the external stress above 150 MPa, ε_R is not sensitive to it and keeps stable at about 1.74%. Under a constant stress, the volume fraction of martensite can be composed of a self-accommodating one and a re-oriented one. In the case of thermomechanical loading, two types of martensite may be created. The recovery strain is proportional to the volume fraction of re-oriented martensite. The insensitivity of ε_R to the stress above 150 MPa indicates that the volume fraction of a re-oriented martensite tends to saturation despite the stress increasing further.

4 Conclusions

1) Amorphous as-spun $Ti_{52}Ni_{23}Cu_{25}$ ribbon is fully crystallized when being annealed at 400 ℃ for 10 h. The annealed ribbon is composed of $B2$, $B19$ and $B11$-TiCu phases with (001) preferential orientation.

2) The transformation of the annealed ribbon detected by DSC exhibits one-stage reversible $B2 \longleftrightarrow B19$ transformation. M_s of the annealed ribbon is 17 ℃ and the transformation hysteresis is as small as 14 ℃.

3) The rearrangement of the martensite variants and stress-induced MT are observed below the M_f temperature and above the A_f temperature, respectively. The elastic modulus in austenite state is about 37 GPa. The annealed ribbon shows up to 1.6% superelasticity shape recovery with low hysteresis of 25 MPa. No obvious flat stress-plateau is associated with the superelasticity.

4) The annealed ribbon exhibits a well-defined shape memory effect during thermal cycling from −60 to 100 ℃. The average value of temperature hysteresis is about 51 ℃ under external stress. ε_M and ε_P both increase with increasing the applied stress. Under the external stress above 150 MPa, ε_R is not sensitive to it and keeps stable at about 1.74%.

References

[1] OTSUKA K, REN X. Physical metallurgy of Ti-Ni-based shape memory alloys [J]. Progress in Materials Science, 2005, 50: 511−678.

[2] MERICIER O, MELTON K N. The substitution of Cu for Ni in NiTi shape memory alloys [J]. Metallurgical Transactions A, 1979, 10: 387−389.

[3] FURUYA Y, MATSUMOTO M, KIMURA H S, MASUMOTO T. Thermoelastic phase transformation of melt-spun $Ti_{50}Ni_{50-x}Cu_x$ (x= 0−20 at.%) ribbons [J]. Mater Sci Eng A, 1991, 147: L7−L11.

[4] NAM T H, SABURI T, SHIMIZU K. Cu-content dependence of shape memory characteristics in Ti-Ni-Cu alloys [J]. Mater Trans JIM, 1990, 31: 959−967.

[5] NAM T H, SABURI T, NAKATA Y, SHIMIZU K. Shape memory characteristics and lattice deformation in Ti-Ni-Cu alloys [J]. Mater Trans JIM, 1990, 31: 1050−1056.

[6] MIYAZAKI S, MIZUKOSHI K, UEKI T, SAKUMA T, LIU Y N. Fatigue life of Ti-50at.%Ni and Ti-40Ni-10Cu (at.%) shape memory alloy wires [J]. Mater Sci Eng A, 1990, 273/275: 658−663.

[7] KIM Y W, NAM T H. The effect of the melt spinning processing parameters on the martensitic transformation in $Ti_{50}Ni_{35}Cu_{15}$ shape memory alloys [J]. Scripta Mater, 2004, 51(7): 653−657.

[8] XIE Z L, CHENG G P, LIU Y. Microstructure and texture development in $Ti_{50}Ni_{25}Cu_{25}$ melt-spun ribbon [J]. Acta Mater, 2007, 55: 361−369.

[9] CHENG G P, XIE Z L, LIU Y. Transformation characteristics of annealed $Ti_{50}Ni_{25}Cu_{25}$ melt spun ribbon [J]. Journal of Alloys and Compounds, 2006, 415: 182−187.

[10] LIU Y. Mechanical and thermomechanical properties of a $Ti_{50}Ni_{25}Cu_{25}$ melt spun ribbon [J]. Mater Sci Eng A, 2003, 354: 286−291.

[11] CHANG S H, WU S K, KIMURA H. Annealing effects on the crystallization and shape memory effect of $Ti_{50}Ni_{25}Cu_{25}$ melt-spun ribbons [J]. Intermetallics, 2007, 15(3): 233−240.

[12] SANTAMARTA R, SCHRYVERS D. Effect of amorphous-crystalline interfaces on the martensitic transformation in Ti50Ni25Cu25 [J]. Scripta Mater, 2004, 50(12): 1423−1427.

[13] SANTAMARTA R, SCHRYVERS D, TWINNED B C C. Spherical particles in a partially crystallized $Ti_{50}Ni_{25}Cu_{25}$ melt-spun ribbon [J]. Intermetallics, 2004, 12: 341−348.

[14] HE W J, TOLOCHKO O V, MIN G H, Y H. Effect of annealing temperature on the transformation characteristics of Ti-rich TiNiCu melt-spun ribbons [J]. Metal Physics and Advance Technology, 2007, 29(9): 1167−1175.

[15] RÖSNER H, SCHLOßMACHER P, SHELYAKOV A V, GLEZER A M. The influence of coherent TiCu plate-like precipitates on the thermoelastic martensitic transformation in melt-spun $Ti_{50}Ni_{25}Cu_{25}$ shape memory alloys [J]. Acta Mater, 2001, 49: 1541−1548.

[16] NAM T H, PARK S M, KIM T Y, KIM Y W. Microstructures and shape memory characteristics of Ti-25Ni-25Cu (at.%) alloy ribbons [J]. Smart Materials and Structures, 2005, 14: S239−S244.

[17] SANTAMARTA R, CESARI E, PONS J, GORYCZKA T. Shape memory properties of Ni-Ti based melt-spun ribbons [J]. Metall Mater Trans A, 2004, 35: 761−770.

(Edited by YANG Bing)